ChemComm

COMMUNICATION

View Article Online
View Journal | View Issue

Cite this: *Chem. Commun.*, 2014, **50**, 10887

Received 30th April 2014,
Accepted 22nd July 2014

DOI: 10.1039/c4cc03234a

www.rsc.org/chemcomm

Structural modeling of iron halogenases: synthesis and reactivity of halide-iron(IV)-oxo compounds†

Oriol Planas,[a] Martin Clémancey,[bcd] Jean-Marc Latour,[bcd] Anna Company*[a] and Miquel Costas*[a]

A structural synthetic model of the iron(IV)-oxo-halide active species of non-heme iron dependent halogenases is reported. Compounds with general formula $[Fe^{IV}(O)(X)(Pytacn)]^+$ (1-X, X = Cl, Br) have been prepared and characterized spectroscopically and chemically with regard to their oxidizing ability. 1-X performs hydrogen-atom abstraction of C–H bonds at reaction rates 2–3 times faster than the corresponding solvato dicationic species, thus modelling the first step in C–H functionalization taking place in natural halogenation.

Biological halogenation of unactivated C–H bonds is catalysed by α-ketoglutarate dependent nonheme iron halogenases.[1] CytC3 and SyrB2 are the best known examples of this type of halogenating enzyme. SyrB2 catalyzes the chlorination of the primary C–H bond of a threonyl residue[2] while CytC3 mediates multiple chlorination of the terminal methyl group in L-aminobutyrate.[3] Spectroscopic and kinetic studies on CytC3 revealed the existence of high-spin Cl–Fe^{IV}=O centers as reactive intermediates.[4,5] These transients are proposed to carry out the functionalization of the substrate through an initial hydrogen-atom abstraction reaction, giving rise to a Cl–Fe^{III}–OH compound and a carbon-centered radical. Then, the rebound of this radical with the chloride ligand affords the chlorinated product. The relative *cis* disposition of the halide ligand with respect to the oxo group is regarded as a key feature that allows the halogenation to take place.[4,6]

While several synthetic models of the iron(IV)-oxo species found in non-heme iron dependent oxygenases have been prepared,[7–9] advances in the modelling of mononuclear nonheme iron halogenases remain modest, presumably because oxo-iron(IV) complexes that contain *cis*-available coordination sites to the oxo ligand are very unstable and scarce. Indeed preparation of synthetic models of the iron(IV)-oxo-halide unit found in these enzymes has only been achieved in two well-defined systems; the low spin $[Fe^{IV}(O)(X)(tpa)]^+$ (X = Cl, Br; tpa = tris(2-pyridylmethyl)amine)[10] and the high spin $[Fe^{IV}(O)(Cl)(TMG_2dien)]^+$ (TMG_2dien = 2′,2′-(2-2′-(methylazanediyl)-bis(ethane-1,2-diyl))bis(1,1,3,3-tetramethylguanidine)).[11] These turned out to be transient short-living species the identity of which has been spectroscopically established. However, reactivity studies to evaluate the ability of these complexes to engage in biologically relevant C–H functionalization and oxygen atom transfer reactions have not been reported. Finally, recent studies point out that coordinatively saturated oxo-iron(IV) complexes engage in electron transfer reactions with halides.[12] Therefore, the oxidation reactivity of a synthetic complex containing the *cis*-Cl–Fe^{IV}=O unit remains to be shown. On the other hand, stoichiometric halide ligand transfer[13] and catalytic[14,15] chlorination of alkanes mediated by iron coordination complexes find some precedent in the literature. High-valent metal oxo species have been proposed to be involved in these reactions on the basis of product analysis and computations,[16,17] but direct evidence for such species could not be gained.

Recently, some of us reported the preparation of an iron(IV)-oxo compound based on the tetradentate ligand 1-(2′-pyridylmethyl)-4,7-dimethyl-1,4,7-triazacyclononane (Pytacn) (Scheme 1).[18] $[Fe^{IV}(O)(Pytacn)(NCMe)]^{2+}$ (**1-NCMe**) exhibits a remarkable stability at room temperature with a half-life time of 2.2 h at 15 °C. Taking advantage of this rather unique stability for an oxo-iron(IV) complex with a *cis*-labile site, in the present work we report the preparation of $[Fe^{IV}(O)(X)(Pytacn)]^+$ (**1-X**, X = Cl, Br) as structural models of non-heme iron halogenases. The stability of these compounds enables their spectroscopic characterization and a detailed

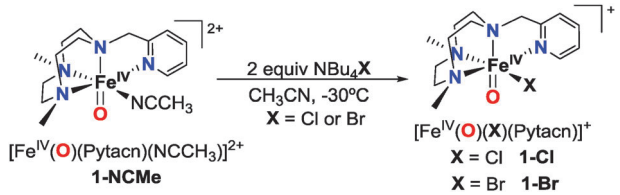

Scheme 1 Preparation of **1-Cl** and **1-Br** from **1-NCMe**.

[a] *Grup de Química Bioinorgànica i Supramolecular (QBIS), Institut de Química Computacional i Catàlisi (IQCC), Departament de Química, Universitat de Girona, Campus Montilivi, E17071 Girona, Catalonia, Spain. E-mail: anna.company@udg.edu, miquel.costas@udg.edu*
[b] *Univ. Grenoble Alpes, LCBM, F-38054 Grenoble, France*
[c] *CNRS, UMR 5249, LCBM, F-38054 Grenoble, France*
[d] *CEA, DSV, iRTSV, LCBM, pmb, F-38054 Grenoble, France*

† Electronic supplementary information (ESI) available: Experimental details and additional data. See DOI: 10.1039/c4cc03234a

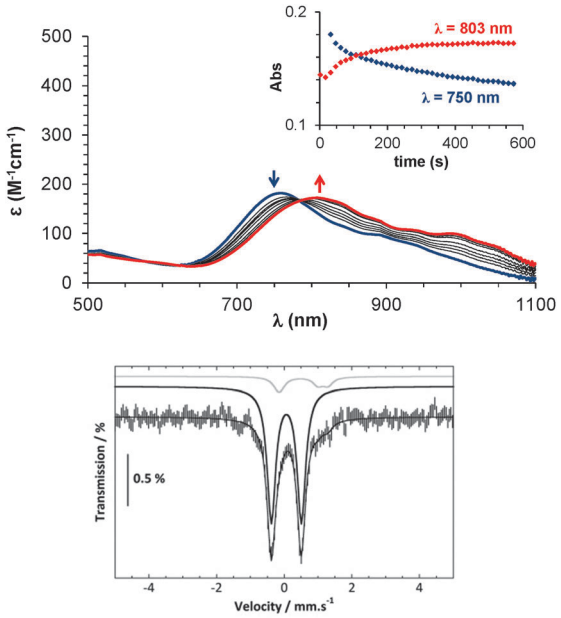

Fig. 1 Top: UV/vis absorption spectra obtained upon reaction of **1-NCMe** with 2 equiv. of NBu_4Cl in acetonitrile at 243 K to give **1-Cl**. Inset: kinetic profile of this process at 750 and 803 nm. Bottom: Mössbauer spectrum of **1-Cl** in acetonitrile recorded at 80 K in zero applied magnetic field. The black sub-spectrum corresponds to the Fe^{IV} ion (see the text) and the gray sub-spectrum to a (μ-oxo)diferric impurity (12%, see ESI†).

study of their reactivity against C–H groups, oxygen atom transfer reactions, and exchange of the oxo ligand with exogenous water.

Compound **1-NCMe** was generated *in situ* in acetonitrile at 288 K by addition of peracetic acid (2 equiv.) to the iron(II) precursor $[Fe^{II}(Pytacn)(NCMe)_2]^{2+}$.[18] Subsequently, 2 equiv. of tetrabutylammonium halide (NBu_4X; X = Cl, Br) were added at 243 K, which led to the new species **1-Cl** and **1-Br** (Scheme 1). Formation of these complexes could be clearly followed by UV/vis spectroscopy by the progressive shift of the characteristic iron(IV)-oxo near-IR band of **1-NCMe** at 750 nm to 803 and 823 nm for **1-Cl** and **1-Br**, respectively. The clean conversion of **1-NCMe** into **1-X** was evidenced by the presence of isosbestic points during these transformations (Fig. 1 top and Fig. S1, ESI†). The red shift of the near-IR band is in accordance with the weaker ligand field exerted by these ligands with respect to MeCN, bromide being a weaker field ligand than chloride.[10] At 243 K **1-Cl** and **1-Br** present half-life times ($t_{1/2}$) of 190 min and 165 min, respectively. The complexes were further characterized by Mössbauer spectroscopy using ^{57}Fe-enriched samples. The spectra recorded at 80 K under zero-applied magnetic field exhibit a doublet which represents 88% of total iron, with a quadrupole splitting (ΔE_Q) of 0.89 mm s^{-1} in both cases, and an isomer shift (δ) of 0.06 mm s^{-1} and 0.07 mm s^{-1} for **1-Cl** and **1-Br**, respectively (Fig. 1 bottom and Fig. S3, ESI†). These parameters are close to those reported for **1-NCMe** (δ = 0.05 mm s^{-1} and ΔE_Q = 0.73 mm s^{-1})[18] and they are consistent with an iron(IV) center in a low spin (S = 1) configuration.[19] High resolution cryospray mass spectroscopy (CSI-MS) of **1-Cl** at 243 K in acetonitrile showed an intense peak at m/z 355.0993 with a mass value and an isotopic pattern fully consistent with $[Fe^{IV}(O)(Cl)(Pytacn)]^+$ (Fig. S2, ESI†). Furthermore, this peak shifted by two units when $H_2{}^{18}O$ was used to generate the **1-NCMe** precursor of **1-Cl**, further confirming the presence of an oxo ligand. Unfortunately, **1-Br** could not be unambiguously characterized by ESI-MS due to the appearance of an interfering peak that prevented its clear identification (m/z = 400.0510). The clean coordination of Cl^- and Br^- to **1-NCMe** contrasts with recent studies showing that selected iron(IV)-oxo systems carry out the $1e^-$ oxidation of halides (Cl^-, Br^-, I^-) to give the corresponding halide radicals.[12] In such cases, the iron center is coordinated to N-based pentadentate ligands and a terminal oxo ligand, so that it presents a coordinatively saturated octahedral geometry. As a result, coordination of halides is prevented and they become potential oxidizable substrates for the iron-oxo unit. Instead, halide anions substitute the labile acetonitrile ligand in **1-NCMe** leaving the iron(IV)-oxo unit intact.

Having established the molecular identity of the complexes, we sought to establish basic aspects of their reactivity. In the first place, exchange of the oxo ligand of **1-Cl** with $H_2{}^{18}O$ (600 equiv.)[18,20] was studied in acetonitrile at 243 K by monitoring over time the ^{18}O-isotopic content of **1-NCMe** and **1-Cl** by means of CSI-MS. While the amount of ^{18}O-labeled **1-NCMe** reaches 18% after 3 hours of reaction with 600 equiv. of $H_2{}^{18}O$, no ^{18}O-exchange occurred with **1-Cl** over the same period of time. Thus, the strong binding of the chloride blocks the labile coordination site, preventing ligand exchange with water and further oxygen-atom exchange of the oxo ligand in the iron(IV) center.

The relative oxygen-atom transfer ability of **1-NCMe**, **1-Cl** and **1-Br** was studied next by analyzing their reaction towards methyl phenyl sulfide (PhSMe) at 243 K. The reaction afforded the corresponding sulfoxide in 76–92% yield (Table S1, ESI†). A kinetic analysis of the reaction could be performed by UV/vis spectroscopy by monitoring the decay of the bands at 750 nm, 803 nm and 823 nm characteristic of the iron(IV)-oxo complexes **1-NCMe**, **1-Cl** and **1-Br**, respectively. Under conditions of excess thioanisole (5–20 equiv. with respect to iron), reactions showed pseudo-first-order behaviour so that the observed reaction rates (k_{obs}) were linearly dependent on substrate concentration (Fig. S5, ESI†). From this analysis, second-order rate constants (k_H) were obtained at 243 K (Table 1). As can be extracted from the k_H values, a subtle effect of the ligand *cis* to the oxo unit on the reaction rate is observed, **1-Cl** being the most reactive complex, followed by **1-Br** and **1-NCMe**. A linear Hammett plot with a negative slope (ρ = −1.0 to −1.5) was obtained by plotting $\log(k_Y/k_H)$ against the Hammett parameter (σ_p), where k_Y is the second-order rate constant corresponding to the reaction with *para*-substituted methyl phenyl sulfides, *p*-Y-thioanisoles (Y = CN, Cl, Me, OMe) (Fig. 2 and Fig. S6, ESI†). This negative value indicates that the oxo group in **1-X** is electrophilic. On the other hand, the small slope (−1.9 to −2.9) obtained by plotting $\log(k_Y)$ with respect to the one-electron oxidation potential of *p*-Y-thioanisoles (E^o_{ox}) indicates that the oxidation occurs *via* a direct oxygen-atom transfer process (Fig. S7, ESI†).[21–24] Further evidence for a direct oxygen-atom transfer from the terminal oxo ligand to the sulfide came from labelling

Table 1 Kinetic parameters for the oxidation of thioanisole and 9,10-dihydroanthracene carried out by **1-NCMe**, **1-Cl** and **1-Br** (determined at 243 K)

	Thioanisole		9,10-Dihydroanthracene	
	k_H (M^{-1} cm^{-1})	ρ	k_2 (M^{-1} cm^{-1})	KIE
1-NCMe	$1.3 \pm 0.1 \times 10^{-4}$	−1.5	$0.81 \pm 0.05 \times 10^{-3}$	27
1-Cl	$3.0 \pm 0.2 \times 10^{-4}$	−1.0	$2.22 \pm 0.06 \times 10^{-3}$	25
1-Br	$1.76 \pm 0.06 \times 10^{-4}$	−1.0	$1.89 \pm 0.06 \times 10^{-3}$	25

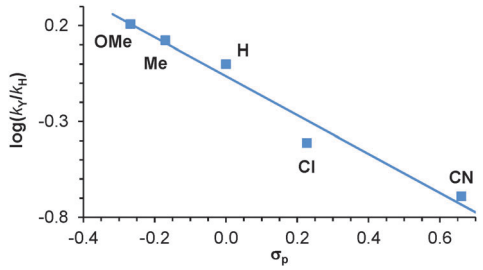

Fig. 2 Hammett plot (determined at 243 K) corresponding to the reaction of **1-Cl** with different *para*-substituted methyl phenyl sulfides (*p*-Y-thioanisoles).

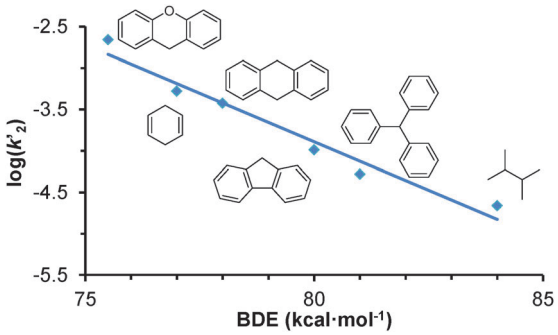

Fig. 3 Plot of log(k_2') (determined at 243 K) against the C–H BDE of different substrates for **1-Cl**.

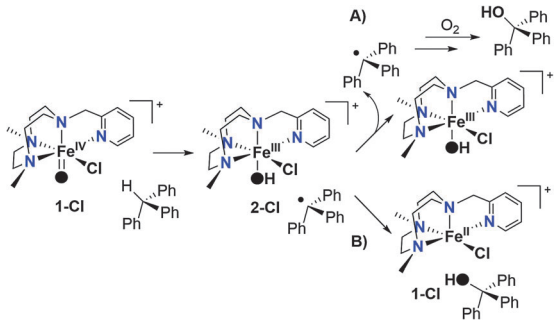

Scheme 2 Mechanistic scheme of the reaction of **1-Cl** with triphenylmethane.

experiments. Thus, reaction of ^{18}O-labeled **1-Cl** (prepared from ^{18}O-labelled **1-NCMe**) with thioanisole afforded 84% ^{18}O-labeled methyl phenyl sulfoxide. In conclusion, **1-Cl** and **1-Br** are good oxo transfer agents. However, their reaction rates towards sulfides are still far from those measured for iron(IV)-oxo complexes with activated oxo ligands, either by protonation[25] or hydrogen-bond formation with second coordination sphere amide functionalities.[26]

The reaction of **1-X** against C–H bonds was first evaluated for the oxidation of 9,10-dihydroanthracene (DHA). Reaction of **1-X** with DHA produced the corresponding polycyclic aromatic hydrocarbon (anthracene) and the oxygenated products anthrone and anthraquinone. No evidence for chlorinated products was obtained. Following the same methodology as described above for the oxidation of sulfides, second-order rate constants (k_2) could be determined (Fig. S9, ESI† and Table 1). Comparison of these reaction rates indicates that **1-Cl** and **1-Br** are between 2 and 3 times more reactive than **1-NCMe** in their reaction with DHA. Albeit significant, the enhancement in oxidation reactivity observed by modifying the *cis*-site to the oxo ligand is relatively modest when compared with *trans*-effects in other oxo-iron(IV) complexes.[27]

More information about the mechanism was obtained by investigating the reaction with a series of substrates having C–H bonds with different bond dissociation energies (BDE). Apart from DHA, xanthene, 1,4-cyclohexadiene (CHD), fluorene, triphenylmethane and 2,3-dimethylbutane (DMB) were used as substrates. Second order rate constants (k_2) for each substrate were adjusted to account for the reaction stoichiometry. This afforded the corrected k_2' based on the number of abstractable weak C–H bonds of substrates (*i.e.* four for DHA and CHD, two for xanthene, fluorene and 2,3-dimethylbutane, and one for triphenylmethane). Rate constants decreased with the increase in the strength of the C–H bond and more interestingly log(k_2') correlated linearly with BDE (Fig. 3 and Fig. S10, ESI†) (slope = −0.23 to −0.30). This good correlation indicates that reactions take place through a hydrogen-atom abstraction (HAT) mechanism, as established earlier for related iron(IV)-oxo compounds.[27–29] Moreover, the measured kinetic isotope effect (KIE), determined by comparison of the reaction rate of DHA and d_4-dihydroanthracene, was found to be around 26 (Table S4, ESI†). Such a high value is consistent with C–H bond cleavage being the rate-determining step and suggests that hydrogen-atom transfer is dominated by quantum mechanical tunnelling.[27]

Thus, reaction of **1-X** with C–H bonds (R–H) entails an initial hydrogen atom transfer, as also proposed for non-heme iron dependent halogenases. In this enzymatic reaction, a carbon-centered radical (R$^\bullet$) is generated in the substrate, concomitant with a LFe^{III}(OH)(X) species **2-X** (Scheme 2). In halogenases, "rebound" of the substrate radical towards the Fe^{III}–X unit results in substrate halide (R–X) formation. The lack of halogenated products in the reaction of **1-X** with C–H bonds[30] may reflect instead two possible scenarios. In the first one, rebound does not take place, and carbon-centered radical intermediates do not react with **2-X**, but instead diffuse in solution and react with other molecules such as adventitious O_2 (Scheme 2, path A). Alternatively, the reaction of the radical with **2-X** occurs exclusively at the Fe^{III}–OH site, leaving the Fe–X (X = Cl, Br) bond intact (Scheme 2, path B). In order to investigate this aspect, reaction of **1-Cl** with triphenylmethane was subjected to isotopic labelling studies and the fate of **1-Cl** after reaction was explored by high resolution ESI-MS. When ^{18}O-labelled **1-Cl** (90% ^{18}O-labelled according to ESI-MS) was reacted with triphenylmethane under a N_2 atmosphere, the corresponding tertiary alcohol is 90% ^{18}O-labelled, in excellent agreement with **1-Cl**. The ESI-MS spectrum of the final reaction mixture is dominated by two ion clusters corresponding to [Fe^{III}(Cl)$_2$(Pytacn)]$^+$ and [Fe^{III}(Cl)(OAc)(Pytacn)]$^+$ (Fig. S11, ESI†), suggesting that the oxo ligand has been transferred to the substrate. Instead, when the same reaction was performed in air, the alcohol is 78% ^{18}O-labelled, and the ESI-MS spectrum shows an additional peak corresponding to **2-Cl**. These observations strongly suggest that a large portion of the alcohol originates from a rebound-like mechanism entailing reaction of the carbon-centered radical and the Fe^{III}–OH moiety. In this scenario, under N_2, **2-Cl** is fully consumed by reaction with the radical, but not in air, because some of the radical is trapped by atmospheric O_2. In both cases, ferric compounds are the final products, presumably because Fe^{II} intermediates formed along path B are rapidly consumed by reaction with excess of oxidant.

Therefore, while **1-Cl** reproduces the key *cis*-Cl–Fe^{IV}=O unit of the active species of non-heme iron dependent halogenases (albeit with a different spin state) and can model the initial C–H bond activation step, subsequent halide transfer does not take place. As reaction of **1-Cl** with C–H bonds appears to occur to a large extent through a rebound-like mechanism (path B), the lack of halogenation products reflects an innate dominant tendency of the radical for the hydroxyl over the halide ligand. This failure may actually have relevance in understanding the enzymatic mechanism. The factors that determine enzymatic halogenation *versus* hydroxylation have been a matter of intense debate. Protonation of the hydroxide ligand,[31] or reaction with CO_2,[32] have been proposed to block this group, preventing its reaction with the carbon-centered radical. On the basis of theoretical calculations, halogenation takes place preferentially because the Fe^{III}–Cl bond is computed to be weaker than the Fe^{III}–OH bond.[33] On the other hand, studies on SyrB2 with non-natural substrates have shown formation of substantial amounts of hydroxylated products, and it has been concluded that SyrB2 favours halogenation in the natural substrate by positioning the reactive C–H group away from the oxo ligand and closer to the halogen.[34] Computational analyses have provided further support for this proposal.[4,35] With **1-Cl** in hand, some of these aspects could be addressed. Indeed, chlorinated products were not observed when the reaction was performed in the presence of 1 equiv. of a strong Brönsted acid, a Lewis acid (Sc^{3+}) or CO_2, all of which aimed at blocking the incipient hydroxide ligand in **2-Cl**.[36]

In summary, we have been able to prepare structural models of the reactive intermediates found in mononuclear non-heme iron halogenases. These compounds behave as oxygen atom transfer agents and also react with C–H groups by means of a HAT reaction. Halide coordination is translated in an increase in the reaction rates both in hydrogen-atom abstraction and oxygen-atom transfer reactions, while it completely inhibits the oxygen-atom exchange with water. However, further reaction of the carbon-centered radical with the *cis*-Fe^{III}(OH)(Cl) species occurs exclusively at the hydroxide ligand, suggesting that this constitutes the most favourable path unless some directing element diverges chemoselectivity. Further studies will be aimed towards integrating directing elements into the oxo-halide-iron species in order to achieve C–H halogenation.

The authors acknowledge the European Commission for project FP7-PEOPLE-2011-CIG-303522 (A.C.), the European Research Council for project ERC-009StG-239910 (M.C.), Generalitat de Catalunya for an ICREA Academia Award (M.C.) and a predoctoral FI fellowship to O.P., and the Spanish Ministry of Science for project CTQ2012-37420-C02-01/BQU (M.C.) and a Ramón y Cajal contract to A.C. J.-M.L. acknowledges the support, in part, of Labex ARCANE (ANR-11-LABX-0003-01). We thank Catexel for a generous gift of tritosyl-1,4,7-triazacyclononane. We are grateful for financial support from INNPLANTA project INP-2011-0059-PCT-420000-ACT1 to Dr X. Ribas.

Notes and references

1 F. H. Vaillancourt, E. Yeh, D. A. Vosburg, S. Garneau-Tsodikova and C. T. Walsh, *Chem. Rev.*, 2006, **106**, 3364–3378.
2 M. L. Matthews, C. M. Krest, E. W. Barr, F. H. Vaillancourt, C. T. Walsh, M. T. Green, C. Krebs and J. M. Bollinger, Jr., *Biochemistry*, 2009, **48**, 4331–4343.
3 D. P. Galonic, E. W. Barr, C. T. Walsh, J. M. Bollinger and C. Krebs, *Nat. Chem. Biol.*, 2007, **3**, 113–116.
4 S. D. Wong, M. Srnec, M. L. Matthews, L. V. Liu, Y. Kwak, K. Park, C. B. Bell, E. E. Alp, J. Y. Zhao, Y. Yoda, S. Kitao, M. Seto, C. Krebs, J. M. Bollinger and E. I. Solomon, *Nature*, 2013, **499**, 320–323.
5 D. P. Galonić, E. W. Barr, C. T. Walsh, J. M. Bollinger and C. Krebs, *Nat. Chem. Biol.*, 2007, **3**, 113–116.
6 M. L. Matthews, C. S. Neumann, L. A. Miles, T. L. Grove, S. J. Booker, C. Krebs, C. T. Walsh and J. M. Bollinger, *Proc. Natl. Acad. Sci. U. S. A.*, 2009, **106**, 17723–17728.
7 A. R. McDonald and L. Que, Jr., *Coord. Chem. Rev.*, 2013, **257**, 414–428.
8 W. Nam, Y.-M. Lee and S. Fukuzumi, *Acc. Chem. Res.*, 2014, **47**, 1146–1154.
9 W. Nam, *Acc. Chem. Res.*, 2007, **40**, 522–531.
10 J. U. Rohde, A. Stubna, E. L. Bominaar, E. Munck, W. Nam and L. Que, Jr., *Inorg. Chem.*, 2006, **45**, 6435–6445.
11 J. England, Y. S. Guo, K. M. Van Heuvelen, M. A. Cranswick, G. T. Rohde, E. L. Bominaar, E. Munck and L. Que, Jr., *J. Am. Chem. Soc.*, 2011, **133**, 11880–11883.
12 A. K. Vardhaman, P. Barman, S. Kumar, C. V. Sastri, D. Kumar and S. P. de Visser, *Chem. Commun.*, 2013, **49**, 10926–10928.
13 T. Kojima, R. A. Leising, S. Yan and L. Que, Jr., *J. Am. Chem. Soc.*, 1993, **115**, 11328–11335.
14 P. Comba and S. Wunderlich, *Chem. – Eur. J.*, 2010, **16**, 7293–7299.
15 D. H. R. Barton, B. Hu, D. K. Taylor and R. U. Rojas Wahl, *J. Chem. Soc., Perkin Trans. 2*, 1996, 1031–1041.
16 M. G. Quesne and S. P. de Visser, *J. Biol. Inorg. Chem.*, 2012, **17**, 841–852.
17 H. Noack and P. E. M. Siegbahn, *J. Biol. Inorg. Chem.*, 2007, **12**, 1151–1162.
18 A. Company, I. Prat, J. R. Frisch, R. Mas-Balleste, M. Guell, G. Juhasz, X. Ribas, E. Munck, J. M. Luis, L. Que, Jr. and M. Costas, *Chem. – Eur. J.*, 2011, **17**, 1622–1634.
19 A. Company, J. Lloret-Fillol and M. Costas, Small Molecule Models for Nonporphyrinic Iron and Manganese Oxygenases, in *Comprehensive Inorganic Chemistry II*, ed. J. Reedijk and K. Poeppelmeier, Elsevier, Oxford, 2013, vol. 3, pp. 487–564.
20 M. S. Seo, J.-H. In, S. O. Kim, N. Y. Oh, J. Hong, J. Kim, L. Que, Jr. and W. Nam, *Angew. Chem., Int. Ed.*, 2004, **43**, 2417–2420.
21 Y. Goto, T. Matsui, S.-I. Ozaki, Y. Watanabe and S. Fukuzumi, *J. Am. Chem. Soc.*, 1999, **121**, 9497–9502.
22 C. V. Sastri, M. S. Seo, M. J. Park, K. M. Kim and W. Nam, *Chem. Commun.*, 2005, 1405–1407.
23 A. Company, G. Sabenya, M. González-Béjar, L. Gómez, M. Clémancey, G. Blondin, A. J. Jasniewski, M. Puri, W. R. Browne, J.-M. Latour, L. Que, Jr., M. Costas, J. Pérez-Prieto and J. Lloret-Fillol, *J. Am. Chem. Soc.*, 2014, **136**, 4624–4633.
24 M. J. Park, J. Lee, Y. Suh, J. Kim and W. Nam, *J. Am. Chem. Soc.*, 2006, **128**, 2630–2634.
25 J. Park, Y. Morimoto, Y.-M. Lee, W. Nam and S. Fukuzumi, *J. Am. Chem. Soc.*, 2012, **134**, 3903–3911.
26 L. R. Widger, C. G. Davies, T. Yang, M. A. Siegler, O. Troeppner, G. N. L. Jameson, I. Ivanović-Burmazović and D. P. Goldberg, *J. Am. Chem. Soc.*, 2014, **136**, 2699–2702.
27 C. V. Sastri, J. Lee, K. Oh, Y. J. Lee, T. A. Jackson, K. Ray, H. Hirao, W. Shin, J. A. Halfen, J. Kim, L. Que, Jr., S. Shaik and W. Nam, *Proc. Natl. Acad. Sci. U. S. A.*, 2007, **104**, 19181–19186.
28 J. Kaizer, E. J. Klinker, N. Y. Oh, J.-U. Rohde, W. J. Song, A. Stubna, J. Kim, E. Munck, W. Nam and L. Que, Jr., *J. Am. Chem. Soc.*, 2004, **126**, 472–473.
29 P. Comba, S. Fukuzumi, H. Kotani and S. Wunderlich, *Angew. Chem., Int. Ed.*, 2010, **49**, 2622–2625.
30 Apart from substrates bearing weak C–H bonds, reactivity of **1-X** with alkanes bearing stronger C–H bonds (such as cyclohexane or cyclooctane) was also studied. Reactions were significantly slower and no chlorinated or brominated products were obtained.
31 S. Pandian, M. A. Vincent, I. H. Hillier and N. A. Burton, *Dalton Trans.*, 2009, 6201–6207.
32 S. P. de Visser and R. Latifi, *J. Phys. Chem. B*, 2009, **113**, 12–14.
33 H. J. Kulik, L. C. Blasiak, N. Marzari and C. L. Drennan, *J. Am. Chem. Soc.*, 2009, **131**, 14426–14433.
34 M. L. Matthews, C. S. Neumann, L. A. Miles, T. L. Grove, S. J. Booker, C. Krebs, C. T. Walsh and J. M. Bollinger, Jr., *Proc. Natl. Acad. Sci. U. S. A.*, 2009, **106**, 17723–17728.
35 H. J. Kulik and C. L. Drennan, *J. Biol. Chem.*, 2013, **288**, 11233–11241.
36 A reviewer has suggested that the lack of halide transfer capability of **1-Cl** with regard to tpa and bispidine iron complexes under catalytic conditions[13,14] may reflect a different inherent reactivity of **1-Cl**. However, when [$Fe^{II}(CF_3SO_3)_2$(Pytacn)] is employed as catalyst under conditions analogous to those of ref. 14, chlorination products are formed.

